AIMS Geosciences, 2 (4): 345-365
DOI: 10.3934/geosci.2016.4.345
Received date 14 July 2016
Accepted date 21 November 2016
Published date 24 November 2016

http://www.aimspress.com/journal/geosciences

Research article

Soil Loss Vulnerability in an Agricultural Catchment in the Atlantic Forest Biome in Southern Brazil

Rafael Gotardo, Gustavo A. Piazza *, Edson Torres, Vander Kaufmann and Adilson Pinheiro

Environmental Engineering Department, Regional University of Blumenau (FURB), 89030-000, Blumenau, Santa Catarina, Brazil

*** Correspondence:** Email: gustavoapiazza@gmail.com; Tel: +55-47-9947-2527

Abstract: This study estimates soil loss vulnerability using field samples and spatial data in a 30 km ^{2} area in the Atlantic forest biome in southern Brazil. The anthropogenic part of the landscape consists mainly of small agricultural properties. Soil loss vulnerability was calculated using adaptations of the universal soil loss equation. The results were compared to sediment data collected during field surveys. Spatial analysis was performed using a geographical information system (GIS) and fine resolution data (1 m). Both field and spatial analyses produced similar results, 5.390 tons of soil loss per year using field data and 5.691 tons per year using GIS. Using soil loss and sediment data related to the Concordia River, we estimate that of all the exported sediment 25% of the lost soil reaches the river. These data are an effective source of information for municipal administrators of the region, which consists of small agricultural catchments (dominated by small properties) that comprise the regional economy. A thematic map was used to determine sub-drainage priority as information for public managers.

Keywords: catchment management; land use; sediment transportation processes

1. Introduction

Catchments have been constantly modified by human activities [1]. The removal of native vegetation to expand agricultural and urban frontiers is one of the main sources of ecosystem degradation, such as erosion. Although soil erosion can be associated with natural phenomena, human activities such as agriculture can accelerate it further [2]. Soil erosion is a serious problem arising from agricultural intensification [3] and urban development [4]. It is a major problem in developing countries [5] that threatens natural resources and even the economy [6]. According to Peter et al. [7], soil erosion negatively affects agricultural productivity, water quality, aquatic ecology, and river morphology. The improper use of land combined with current climate anomalies increases soil loss. The soil loss rate is affected by topography, climate, soil characteristics, and vegetation cover [8–11], all of which are affected by human activities [12]. Unprotected areas in particular tend to suffer from erosion.

Soil loss is a diffuse and complex process in catchments that leads to the loss of nutrient-rich surface soil, increased runoff from more impermeable subsoil, and decreased water availability to plants [3]. These processes can be easily qualitatively and quantitatively estimated under a wide range of conditions using current technology. Spatial and quantitative information about soil erosion contributes significantly to soil conservation, erosion control, and general management [13]. The quality processes are determined by taking sediment samples and collecting turbidimeter data, and the quantity is determined using geographic information systems (GIS). Several studies have used the combination of GIS and the universal soil loss equation (USLE) to simulate the impact of land use in catchments [13,14]. The USLE [8] is a simple model for predicting erosion that estimates long-term average annual soil loss and can be modified for specific conditions. The method as a whole is based on estimating soil loss per unit area and takes into account parameters such as precipitation, topography, soil erodibility, erosivity, and runoff [15].

Despite its recognized limitations [16] the USLE model remains one of the most used tools in soil loss modeling for catchments [17]. The simplicity of the methodology can be considered its most important characteristic considering the speed of the changes in both the land use and the climate in the current scenario. Complex models can sometimes be difficult to use due to the parameters, which in some cases can be hard to obtain. The data required for the simple USLE equation can be generated using geospatial techniques [5]. The combined application of USLE and GIS results in a map showing the spatial distribution of potential erosion and is an important tool to support planning and management [18,19]. Advanced image processing techniques have opened up new possibilities for mapping landscape features and thus facilitate quantitative assessments of soil erosion risks [20] that are useful in the planning and conservation of watersheds. Mati and Veihe [21] and Angima et al. [22] state that USLE is the most efficient tool to estimate soil erosion loss and guide development and conservation plans to control erosion under different land-cover conditions. Estimating soil loss and identifying areas where it is critical to implement best management practices is central to the success

of soil conservation programs [3,5]. A quantitative assessment [23] is needed to determine the extent and magnitude of soil erosion problems so that sound management strategies based on field measurements can be developed on a regional basis. The thematic map allows the identification of vulnerable areas where the replacement of natural vegetation with a new use may result in environmental damage. These results can be used as a source of information when implementing land conservation practices that can lead to natural resilience and the proper use of land and water.

In most cases in southern Brazil, there is no measured soil loss data available for agencies to implement watershed management plans. The objective of this work is to estimate soil loss in the Concordia River catchment using the USLE in order to prove its efficiency and ease of use and to demonstrate the potential use of the methodology when no data is available.

2. Materials and Methods

2.1. Study Area

The study was performed in the experimental catchment of the Concordia River (Figure 1) located in Lontras, Santa Catarina, southern Brazil. The Concordia River is a tributary of the Lontras River, which feeds the Itajai-Açu River, the largest watershed on the Atlantic side of the state. The Concordia catchment has a drainage area of 30.93 km². The climate of the region is temperate–humid with hot summers (Cfa according to the Köppen climate classification system) [24] and temperatures reaching above 22 °C. Annual rainfall varies from 1600 to 1800 mm. Cambisol and Red-Yellow Ultisol are the predominant soil types [25]. The catchment is covered by dense ombrophilous forest [26] that is part of the Atlantic Forest biome, in 45.1% of the catchment. The agricultural areas make up 15.7% of the catchment. The main agricultural products are maize, beans, tobacco, and rice. Most farmers adopt the conventional tillage system consisting of subsoiling and plowing.

During 2008, we took soil samples from a 135 scattered points in a shallow soil profile (0–20 cm) within the catchment area (Figure 1). Physical and chemical analyses of the soil were performed at the Environmental Chemistry Laboratory at the State University of Western Paraná (UNIOESTE-PR).

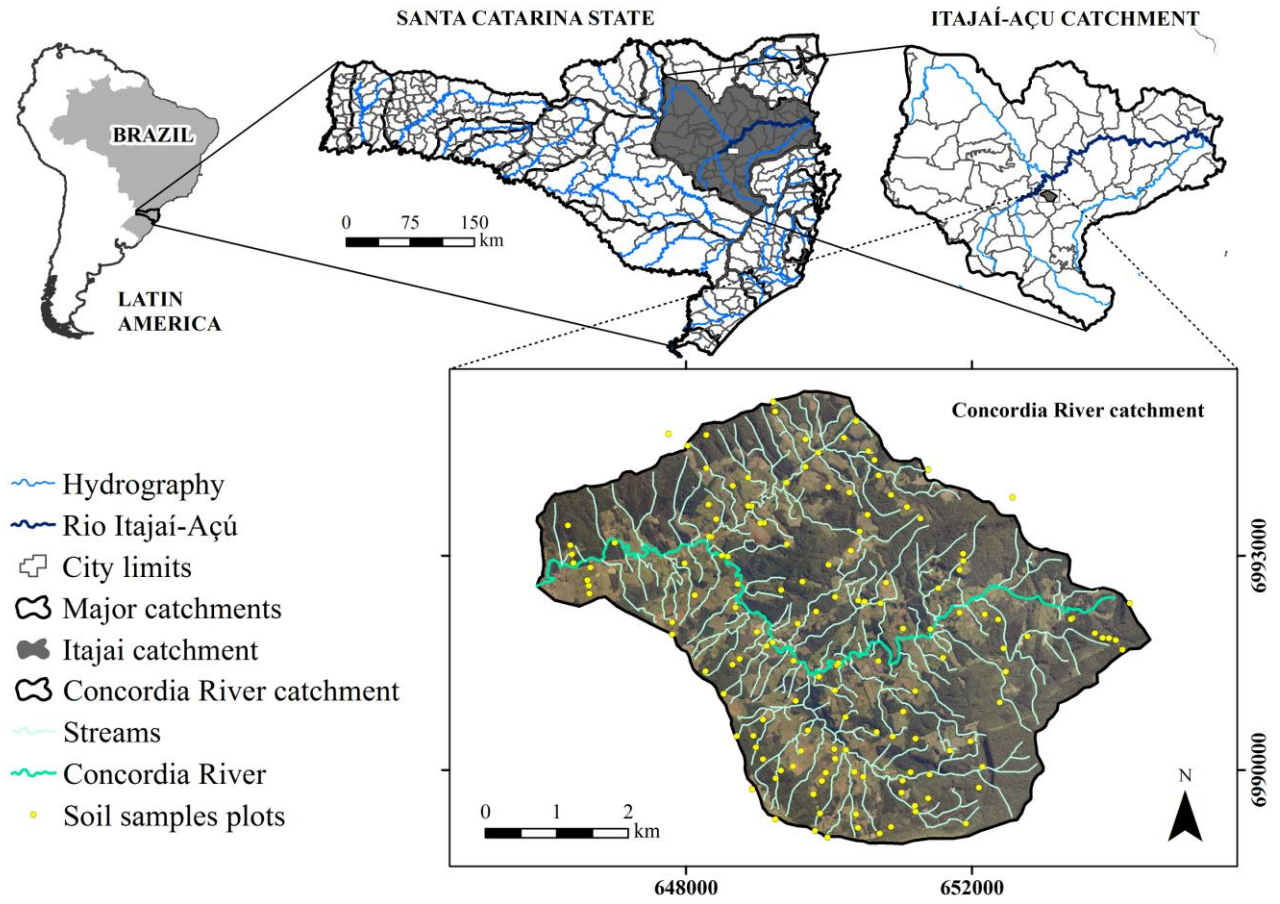

Figure 1. Location map and soil collection plots in Concordia River catchment, Lontras (SC).

2.2. Universal Soil Loss Equation (USLE)

Soil loss was calculated using the USLE for all sample points in the catchment. USLE [27] is an empirical model used to estimate the average loss of soil due to laminar erosion over long periods. The equation is given by:

$$A = R \,.K.LS.C.P \tag{1}$$

Where A is the soil loss ($t \cdot ha^{-1} \cdot yr^{-1}$); R is the rainfall erosivity index; K is the soil erodibility; LS is the topographic factor; C is the plant cover factor; and P represents the specific erosion control practices.

The rainfall erosivity factor (R) is a measure of the erosive force of a specific rainfall. It is generally determined as a function of the intensity and duration of a rainfall. According to Wischmeier and Smith [27], R reflects the effect of rainfall intensity on soil erosion. In this study, monthly and annual rainfalls were used. The annual erosivity was based on the equation (2) created by Renard and Freimund [28] that is designed to simulate the rain energy index in the United States. However, other authors, such as Kim et al. [29] and Markose et al. [5], have used the same equation

in hot and humid regions with conditions similar to those in the Concordia catchment. The monthly rainfall calculation was performed based on the equation (3) created by Bertoni and Lombardi Neto [30]:

$$R = 587.8 - 1.219 \times P + 0.004105 \times P^2 \quad (2)$$

$$R_{monthly} = \sum_{i=1}^{4} 89.823 \times \left(\frac{P_m^2}{P}\right)^{0.759} \quad (3)$$

Where $R_{monthly}$ is the monthly rainfall erosivity (MJ mm ha^{-1} h^{-1}); P_m is the average month precipitation (mm); and P is the annual precipitation (mm).

The soil erodibility (K) represents the vulnerability of soil or surface material to erosion and the amount of runoff given a particular rainfall input, as measured under standard conditions. It is also considered to represent the rate of soil loss per unit of rainfall erosion index for a specific soil. It indicates the vulnerability to erosion in accordance with properties inherent to the land [30]. The soil erodibility was estimated using the Denardin [31] equation (4):

$$K = 7.48x10^{-6}M + 4.48059\times10^{-3}P - 6.31175\times10^{-2}DMP + 1.039567\times10^{-2}N \quad (4)$$

Where K is the erodibility index (MJ $ha^{-1}\cdot mg^{-1}\cdot mm^{-1}$); M is (fine sand + gravel) × [(fine sand + silt) + gravel] (%); P is the permeability factor (dimensionless); N is [gravel × (organic matter content / 100)]; and DMP is weighted average diameter (mm) smaller than 2 mm, expressed by equation (5):

$$DMP = \left[\left(0.65\times A_g\right) + \left(0.15\times A_f\right) + \left(0.0117\times S\right) + \left(0.00024\times a\right)\right]/100 \quad (5)$$

Where A_g is gravel (%); A_f is fine sand (%); S is silt (%); and a is clay (%).

Soil permeability is the process by which water percolates through the soil pores [32]. Permeability can be classified according to the physical and structural characteristics of the soil [33] and the texture. For permeability classification, we used Table 1 from Galindo and Margolis [33].

Table 1. Permeability classification according to soil texture.

Texture	Granulometry	Structure	Permeability class	Factor
Clay	Clay ≥ 35%	Low	Low	3
		Moderate	Low	3
		Strong	Moderate	2
Moderate	15% ≤ clay ≤ 35%	Low	Moderate	2
		Moderate	Moderate	2
		Strong	Quick	1
Sandy	Clay + silt ≤ 15%	Low	Moderate	2
		Moderate	Quick	1
		Strong	Quick	1

Source: Adapted from Galindo e Margolis [33].

The topographic factor is related to the slope steepness factor (*S*) and the slope length factor (*L*) and is considered a crucial factor in quantifying erosion due to surface run-off. The slope has a major effect on the rates of soil erosion. As the slope gets steeper, the higher the velocity of the overland flow becomes, thus increasing shear stresses on the soil particles [34]. Moreover, as the slope length increases, the overland flow and the flow velocity also steadily increase, leading to greater erosion of the soil surfaces [35]. The topographic factor (*LS*) is expressed by the equation proposed by Wischmeier and Smith [27], which defines soil loss due to the length and slope. We used equation (6) to determine the topographic factor:

$$S = \left(\frac{Le}{22.1}\right)^{m} \times (0.065 + 0.04 \times Sd + 0.0065 \times Sd^2) \quad (6)$$

Where *LS* is the topographic factor (dimensionless); *m* is described in Table 2; *Le* is the equivalent rectangle width (m); and *Sd* is the average slope of the basin (%).

The l_e variable was obtained based on Paiva and Paiva [36], determined by equation (7):

$$l_e = \frac{k_c \times \sqrt{A}}{1.128} \times [1 - \sqrt{1 - \left(\frac{1.128}{k_c}\right)^2} \quad (7)$$

Where k_c is the watershed compactness coefficient (dimensionless) and *A* is the catchment area (m^2). The k_c depends on the area and the perimeter of the catchment, described by equation (8):

$$k_c = 0.282 \times Per/\sqrt{A} \quad (8)$$

Where *Per* is the perimeter of the catchment (m) and *A* the area (m^2). The m of the *LS* calculation is assigned according to the average slope, according to Table 2.

Table 2. Values assigned to m variable according to slope.

Slope (*Sd*)	*m*
$Sd < 1\%$	0.2
$1\% \leq Sd \leq 3\%$	0.3
$3\% < Sd\ 5\%$	0.4
$Sd \geq 5\%$	0.5

The average slope (*Sd*) was obtained using the Williams and Berndt [37] equation (9):

$$Sd = 0.25 \times Z \times (LC_{25} + LC_{50} + LC_{75})/A \quad (9)$$

Where Z is the gap between the outflow and the highest altitude (m); LC_{25} is the length of the river considering the elevation lines until 25% of Z (m); LC_{50} is the length of the river considering the elevation lines until 50% of Z (m); LC_{75} is the length of the river considering the elevation lines until 75% of Z (m); and A is the catchment area (m^2).

The plant cover factor (*C*) is the soil loss ratio considering the land use. In this study, values were assigned based on the literature (Table 3).

Table 3. Plant cover factor (*C*) considering the land use.

Land use	*C* factor	Source
Agriculture	0.1097	Bertol et al. [38]
Native Forest	0.002	Martins et al. [39]
Regeneration	0.01	Stein et al. [40]
Pasture	0.01	Tomazoni et al. [41]
Planted Forest	0.008	Martins et al. [39]
Constructed areas	0.01	Morgan [42]
Water bodies	0.0	Stein et al. [40]
Bare soil	1.0	Werneck Lima et al. [17]

The specific erosion control practices (*P*) represent the relationship between the soil loss and the management practices of the region [43]. Practice factor (*P*) is defined as the ratio of soil loss after a specific support practice to the corresponding soil loss after up-and-down cultivation. One of the most common approaches to calculating the specific factor is the evaluation of current farming practices by experts, either with field observations or using aerial photos [44]. In this study, both analysis (field and aerial) were performed. *P* values were assigned according to Table 4.

Table 4. *P* values to different conservation practices.

Conservation practices	Valor de *P*
Permanent green cords (forests)	0.2
Toggle weeding and planting wrap	0.4
Planting in contour	0.5
Downhill planting	1.0
Built-up areas	1.0
Bare soil	1.0
Others	1.0

Source: Wanielista [45] and Werneck Lima et al. [17].

2.3. Universal Soil Loss Equation (USLE) in GIS

When assessing erosion risk at the local and regional levels, GIS become important and powerful tools [46]. According to Mati and Veihe [21], the application of GIS has increased in the last decade with the availability of digital data, cheaper and more user-friendly software, and the need to handle large spatial databases. Multi-temporal, high-resolution, remotely sensed data and GIS have been used extensively to monitor environmental changes and to map land cover changes on local, regional, and global scales [47–49]. These have helped in land use planning and the sustainable management of resources [50,51].

Using GIS, the potential erosion of the catchment was estimated with the help of ArcGIS 10.3. The equation was executed using spatial information about the Concordia catchment, such as GPS points and drainage vectors. Aerial photogrammetric products (elevation, surface, and imagery) with 1-meter resolution of the place were also used. However, for processing purposes all data were processed with spatial resolution of 10 meters in raster format because not all information has the same resolution. Rainfall erosivity (*R*) was calculated using 10 pluviographs located in the study area. For this study, rain gauges were separated according to different altitude classes (300–450, 450–600, 600–750, and 750–900 meters). Each soil sampling point (135) received an *R* value referring to its altitude. An erosivity raster for each season (summer, fall, winter, and spring) was created using the geostatistical analyst tool from ArcGIS using the Kriging interpolation method.

The erodibility (*K*) was obtained based on soil samples of the catchment and the granulometric composition of the soil. A triangulated irregular network (TIN) was created with spatialized values of samples. The topographic factor (*LS*) was calculated based on the digital elevation model (DEM) from the aerial photogrammetric survey. The fill, flow direction, and flow accumulation tools were run, and the slope of the catchment was generated, using the MapAlgebra tool (Raster Calculator) in processing the equation (10). The LS raster was generated following this:

$$LS = \left(\frac{"flow_{acc}" * [spatial.resolution]}{22.1}\right)^{0.4} * (Sin("slope" * 0.01745)/0.09)^{1.4} \quad (10)$$

A simplified classification was executed to derive the plant cover factor (*C*) and specific erosion control practices (*P*). Using color aerial photography (RGB) through the image classification tool, classes of samples were selected: Native Forest/Forestry, Agriculture/Pasture, and Bare Soil/Urban. The maximum likelihood classification algorithm was used. Conversion tools were used to join classes (polygons) in single information for subsequent insertion of *C* and *P* values in the attribute table (Table 5).

Table 5. *C* and *P* values for geoprocessed data.

Land use	*C*	*P*
Native Forest/Planted forest	0.002	0.2
Pasture/agriculture	0.1	0.5
Bare soil/urban	1.0	1.0

With all USLE variables (*R*, *K*, *LS*, *C*, and *P*) we used the Raster Calculator tool to estimate potential erosion in each cell (pixel resolution 10 m × 10 m) in the catchment. With the thematic map performed, vulnerability classes were reclassified using the automatic classifying tool from ArcGIS 10.3 through the Geometrical Interval method. This method creates class breaks based on class intervals that have a geometric series. The geometric coefficient in this classifier can change once (to its inverse) to optimize the class ranges. The algorithm creates geometric intervals by minimizing the sum of squares of the number of elements in each class. This ensures that each class range has approximately the same number of values with each class and that the change between intervals is fairly consistent.

2.4. Sediment Transportation in the Main River

Stream sediment transportation in a catchment is reflected by the presence of particulate matter in suspended form as well as at the bottom of the river. The suspended material consists of the finest fraction of the sediment carried by the turbulent fluid action, which prevents the deposition of the material. The transportation of the bottom material or drag sediment occurs when the hydraulic conditions exceed the critical condition of the bed material. According to Yang [52], the transported sediment in a riverbed can represent up to 25% of the total transported material.

In this study, suspended sediment load estimation for the river was calculated using turbidity and river flow data. A multiparametric probe installed in the catchment outflow collected the turbidity data from 2012 and 2013 with record intervals of 30 minutes. The flow rate was obtained using electronic equipment using the flow data (Thallimedes, OTT®) with a resolution of 0.01 m and precision of ±0.002 mm with data logging intervals of 30 minutes. Both pieces of equipment were installed in the same location. The level data were transformed into flow data using the following equation (11):

$$Q = -1.31250E-05H^3 + 1.61219E-02H^2 - 6.60348E+00.H + 9.03166E+02 \quad (11)$$

Where Q is the flow ($L \cdot s^{-1}$) and H is the water level (cm).

During this period, observations were also made after water sampling analysis of suspended solids in the laboratory that allowed the construction of a curve between suspended solids and turbidity. Using the defined curve, we analyzed the correlation between sediment concentration ($mg \cdot L^{-1}$) and turbidity (NTU), resulting in the equation y = 0.761 + 0.197y with an $R^2 = 0.999$. Suspended soil loss was calculated using the equation.

The bottom soil loss was held by direct measurements in field and mathematical calculations. Bottom sediment samples were used to determine the particle size characteristics. Analysis was performed in the laboratory according to the EMBRAPA Solos Analysis Methods Manual [53]. Initially, we calculated the average particle diameter of the bottom sediment. Following this and using Yang's method (1973), we estimated the bottom outlet. Following are the equations described in Paiva and Paiva [36] for applying Yang's [54] method:

(a) Speed on friction particles (U), equation (12):

$$U = 9.81.Rh.S^{0,5} \quad (12)$$

Where U is the frictional speed ($m \cdot s^{-1}$); Rh is the hydraulic radius of the section (m); and S is the water line slope ($m \cdot m^{-1}$). Consider

(b) Particles fall viscosity (w), equation (13):

$$W = \frac{\left\{\left[\left(\frac{2}{3}\right).g.\left(\frac{\gamma_s}{\gamma}-1\right).D^3 + 36.v^2\right]^{0,5} - 6.Y\right\}}{D} \quad (13)$$

Where W is the particle fall velocity ($m \cdot s^{-1}$); g is the gravitational acceleration ($m \cdot s^{-1}$); D is the particle diameter (m); Y is the kinematic viscosity ($m^2 \cdot s^{-1}$); γs is the specific gravity of water ($t \cdot m^{-3}$); and γ is the specific weight submerged sediment ($t \cdot m^{-3}$).

(c) Critical speed (U_c), equation (14):

$$U_c = W.\left\{\left(\frac{2.5}{\left[\log\left(\frac{U}{D.Y}\right) - 0.06\right]}\right) + 0.66\right\} \quad (14)$$

Where U_c is the critical speed; W is the particle fall velocity ($m \cdot s^{-1}$); D is the particle diameter (m); Y is the kinematic viscosity ($m^2 \cdot s^{-1}$); and U is the speed of friction particles.

(d) Total concentration (TC), equation (15):

$$\log TC = 6{,}681 - 0{,}633.log\left(\frac{W}{D.Y}\right) - 4{,}816.\log\left(\frac{U}{W}\right) + \left[2{,}784 - 0{,}305.log\left(\frac{W.D}{Y}\right) - 0{,}282.log\left(\frac{U}{W}\right)\right].log\left(\frac{U.S}{W} - \frac{U_c}{W}\right) \quad (15)$$

Where TC is total concentration; U_c is the critical speed; W is the particle fall velocity ($m \cdot s^{-1}$); D is the particle diameter (m); Y the kinematic viscosity ($m^2 \cdot s^{-1}$); and U is speed of friction particles.

(e) Solid sediment discharge (Qt), equation (16):

$$Qt = 0.0864.Q.CT \quad (16)$$

Where Qt is the total discharge ($t \cdot day^{-1}$); Q flow ($m^3 \cdot s^{-1}$); and CT is sediment concentration ($mg \cdot L^{-1}$).

3. Results and Discussion

3.1. USLE Factors

For the Concordia River, the greatest soil loss happens in the summer season, considering the rainfall; soil loss reaches 0.789 $t \cdot ha^{-1} \cdot yr^{-1}$. The next greatest soil loss occurs in spring, at 0.509 $t \cdot ha^{-1} \cdot yr^{-1}$. In winter, there is a soil loss of 0.438 $t \cdot ha^{-1} \cdot yr^{-1}$, and in fall there is a soil loss of 0.426 $t \cdot ha^{-1} \cdot yr^{-1}$. This result can be explained by the intensity and volume of rainfall that occurred during summer, which is greater compared to the other seasons (Table 6). Studying the erodibility of Cambisol during rainfall, Bertol et al. [38] also observed greater soil losses during the spring and summer seasons.

Table 6. Soil loss seasonality of Concordia River catchment—Lontras (SC).

Season	Average Rainfall (mm)	Soil Loss ($t \cdot ha^{-1} \cdot yr^{-1}$)	Soil Loss ($t \cdot catchment^{-1} \cdot yr^{-1}$)
Summer	600.9	0.789	2,439.6
Fall	422.2	0.426	1,316.5
Winter	407.6	0.438	1,355.4
Spring	475.1	0.509	1,573.0
Total	**1,905.8**	**2.160**	**6,684.2**

The greatest soil loss (2.60 $t \cdot ha^{-1} \cdot y^{-1}$) occurs with typical aluminic Haplic Cambisol (Table 7). In sequence, losses are distributed among typical aluminc Humic Cambisol with 1.99 $t \cdot ha^{-1} \cdot yr^{-1}$, typical aluminic Red-Yellow Ultisol with 1.94 $t \cdot ha^{-1} \cdot yr^{-1}$ and typical aluminic Haplic Cambisol with 1.31 $t \cdot ha^{-1} \cdot yr^{-1}$. The lowest soil loss occurs with Ta typical distrophic Haplic Gleysol with

0.57 t·ha^{-1}·yr^{-1}. It is important to highlight that greater soil losses occur in the summer (Figure 2).

Table 7. Soil loss in different soils of Concordia River catchment—Lontras (SC).

Soil	Type	Area (km^2)	Area (%)	Pha	PB	Specific loss (Pha/area)
Ultisol Red-Yellow typical aluminic	PVAa	9.5	30.9	1.9	1,854.4	0.20
Haplic Cambisol typical aluminic	CXa	13.9	44.9	2.6	3,604.7	0.19
Haplic Cambisol ta typical dystrophic	CXvd	5.0	16.2	1.3	657.6	0.26
HumicCambisol typical aluminc	CHat	1.9	6.3	2.0	388.9	1.02
Haplic Gleysol Ta typical distrophic	Gxva	0.5	1.7	0.6	30.9	1.06
Total	**–**	**30.9**	**100**	**8.4**	**6,536.52**	**0.27**

Legend: Pha: Soil loss per hectare (t·ha^{-1}·yr^{-1}); PB: Soil loss in the catchment (t·catchment^{-1}·yr^{1}).

However, specific soil loss rates (Pha/area) show that the Haplic Gleysol (1.05 t·ha^{-1}·yr^{-1}·km^{-2}) and Humic Cambisol (1.02 t·ha^{-1}·yr^{-1}·km^{-2}) have the highest soil loss vulnerability. These two soils types have the highest potential for soil loss and therefore require more care during management.

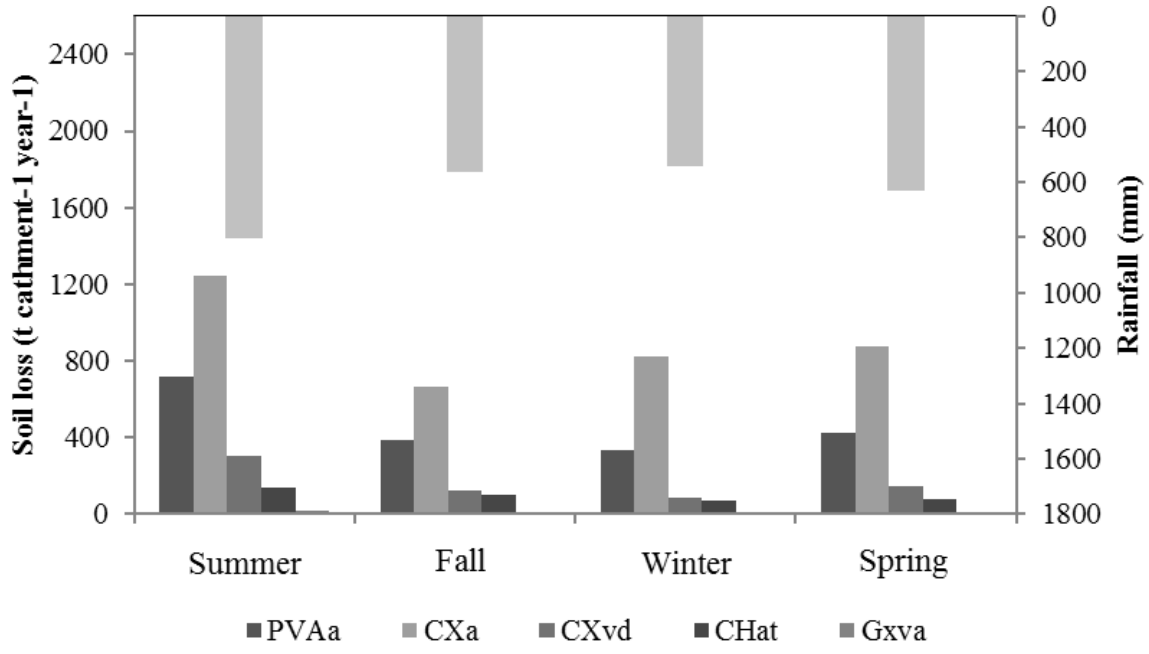

Figure 2. Seasonal soil loss for different soil types of Concordia River, Lontras (SC), Brazil.

Agriculture areas have the highest soil loss in the catchment at with 3043.9 t·catchment^{-1}·yr^{-1}. Native forest areas have the second highest loss at 1482.1 t·catchment^{-1}·yr^{-1}. This is because the native forest comprises the largest part of the catchment, at 45.1% of the total area. In sequence, losses are divided among pasture (404.8 t·catchment^{-1}·yr^{-1}) and planted forest (405.4 t·catchment^{-1}·yr^{-1}).

Regeneration (which comprises the smallest area) is responsible for soil losses of 54.3 t·catchment^{-1}·yr^{-1} (Table 8). However, considering specific losses, regeneration is responsible for the second highest soil loss, reaching 1.1 t·ha^{-1}·yr^{-1}·km^{-2}, following only agriculture with an estimated loss of 1.3 t·ha^{-1}·yr^{-1}·km^{-2}. Native forest areas had the lowest soil loss at 0.076 t·ha^{-1}·yr^{-1}·km^{-2}. Following this was pasture land at 0.1 t·ha^{-1}·yr^{-1}·km^{-2} and planted forest at 0.2 t·ha^{-1}·yr^{-1}·km^{-2}. Regeneration areas may have this result because of the simplified soil and tree structure, which predispose them to erosion.

Table 8. Annual soil loss related to land uses of Concordia River catchment, Lontras (SC), Brazil.

Land use	Area (km^2)	Area (%)	Soil Loss (t·ha^{-1}·yr^{-1})	Soil Loss (t·catchment^{-1}·yr^{-1})	Specific Soil Loss (Soil Loss/area)
Agriculture	4.84	15.65	6.3	3,043.9	1.3
Pasture	5.43	17.54	0.7	404.8	0.1
Native Forest	13.95	45.11	1.0	1,482.1	0.1
Regeneration	0.72	2.32	0.8	54.3	1.1
Planted forest	4.47	14.44	0.9	405.4	0.2
Others	1.18	3.81	–	–	–
Water	0.34	1.11	0	0	0.0
Total	**30.93**	**100**	**9.6**	**5,390.5**	0.3

Analyzing SWAT model response to estimate sediment production in the experimental catchment of the Canchim River (EMBRAPA Pecuária Sudeste), Silva et al. [55] found total sediment losses of 5.7 t·ha^{-1}·yr^{-1}. Their result is low compared to the Concordia River catchment, which had losses of 9.7 t·ha^{-1}·yr^{-1}. Further results were not possible because the authors did not characterize the Canchin catchment properly. Bertoni and Lombardi Neto [30] also estimated soil losses relating to land use in the state of São Paulo and found annual soil losses of 12.4 t·ha^{-1} for sugarcane plantations, 0.9 t·ha^{-1} for orange groves, 12 t·ha^{-1} for corn, 0.4 t·ha^{-1} for pasture land, and 0.9 t·ha^{-1} for planted forest. These values are similar to those in this study in which the greatest losses also occurred for agriculture, pasture land (0.75 t·ha^{-1}), and planted forest (0.91 t·ha^{-1}). The Concordia River catchment results were not similar to Silva's [56] results; he calculated the soil loss in the Canchim catchment using geoprocessing and the USLE model and obtained values of 0.39 t·ha^{-1} for native forest; 2.9 t·ha^{-1} for planted forest; 3.86 t·ha^{-1} for grazing land; 32.5 t·ha^{-1} for sugarcane plantations; and 42 t·ha^{-1} for corn. In a case study of the Coruja/Bonito catchment, which has an area of 52 km^2 in the southern state of Santa Catarina, Vieira [57] found losses of 5,225 t·catchment^{-1}·yr^{-1}, which is similar to the Concordia catchment results (5390.5 t·catchment^{-1}·yr^{-1}).

3.2. GIS

The total soil loss from the catchment is 5691.98 t·yr^{-1}. The Concordia River catchment has greater soil losses in agricultural, pasture, bare soil, and sloped areas (Figure 3). These results are in agreement with those of Oliveira et al. [58], who studied soil vulnerability in the Green River catchment and who found that agricultural and pasture areas have the most erosion.

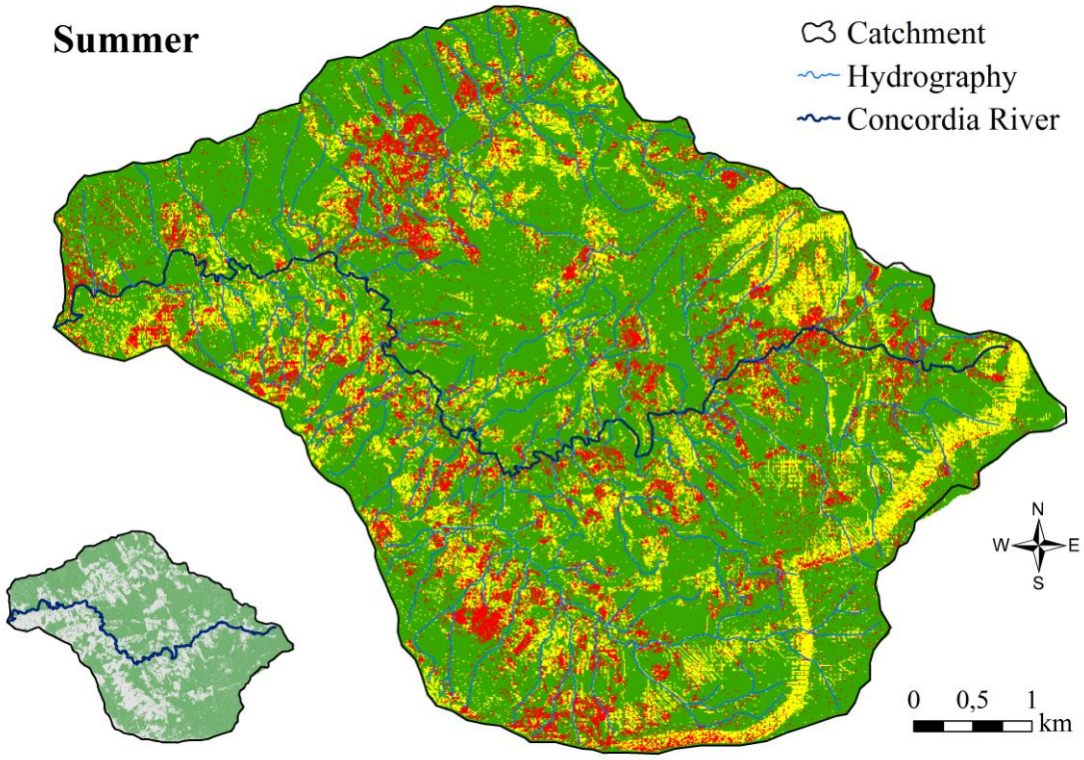

Vulnerability ■ Low, ■ Moderate e ■ High.

Figure 3. Vulnerability map of Concordia River catchment, Lontras (SC), Brazil.

Table 9. Annual soil losses of Concordia River catchment using GIS.

Vulnerability	Summer	Fall	Winter	Spring
Low (0–5 t·catchment^{-1}·yr^{-1})	69.03%	73.88%	74.87%	73.19%
Moderate (5–100 t·catchment^{-1}·yr^{-1})	18.66%	17.50%	16.61%	17.28%
High (>300 t·catchment^{-1}·yr^{-1})	12.31%	8.62%	8.53%	9.53%

The largest amount of soil loss in the catchment occurs in the summer season (Table 9). Urban and bare soil areas combined comprise those areas with the largest soil losses (elevate values of *C* and *P* factor). The Concordia River catchment contains 72.74% of the areas with low vulnerability,

17.51% of the areas with moderate vulnerability, and 9.75% of the areas with high vulnerability. As seen in Figure 3, the majority of the study area experiences soil erosion between 0 and 5 t·catchment year^{-1}, especially where the slope is very low. However, excessive soil erosion is observed in downstream areas of the catchment where heavy rainfall events make ideal conditions for soil loss. High erosion rates are associated with either a higher slope gradient or with degraded bare land, grassland, or shrub land cover.

Studying the Yialias River in the Potamia catchment (110 km^2) in the broader region of Nicosia, Cyprus, Alexakis et al. [34] found soil losses of 6,391 t·ha^{-1}·year^{-1}. Pradeep et al. [59] determined soil erosion rates (ranging from 0 to 4227 t·h^{-1}·year^{-1}) of sub-watersheds of the Meenachil River in India using the RUSLE model. The estimated soil loss for the study area varied from 0 to 6995 t·ha^{-1}·year^{-1} (with the greatest occurrence of 0 and 49 t·ha^{-1}·year^{-1} classes). Ganasri and Ramesh [3] estimated annual soil losses of 473,339 t·yr^{-1} in the Nethravathi Basin (3128.72 km^2) in India using the RUSLE model.

3.3. Sediment Load Estimation for the Concordia River

The annual sediment transported in suspension is 698.7 t·yr^{-1}. Suspended solids ranged from 76.57 t for spring to 318.04 t for winter (Table 10). This result can be attributed to the agricultural practices of the region based on conventional tillage of the soil leading to exposure (bare soil). According to Gilles et al. [60], conventional tillage leaves the soil with no cover, thus reducing roughness and porosity and increasing vulnerability to erosion. The bottom transportation of sediments, however, was higher in summer due to the precipitation that raised the river level and thereby increased the transport of solid particles.

Table 10. Production and export of sediments of Concordia River catchment.

Season	Rainfall (mm)	Flow (m^3/s)	Total Soil loss–USLE (t·catchment^{-1}·yr^{-1})	Suspended solids–River (Turbidimeter)	Bottom sediment (Yang, 1973)	Total transported sediments
Summer	621.03	2.45	2,654.6	151.9	321.4	473.3
Fall	428.23	1.83	1,612.5	177.1	283.1	406.4
Winter	417.03	3.24	1,685.7	318.0	306.3	624.4
Spring	442.43	1.04	1,281.1	76.6	145.9	190.3

3.4. First Attempt at an Erosion Management Map for Concordia River

USLE results show that erosion occurs in the zone between 300 and 800 m elevation. It is essential to focus conservation efforts in this zone. In order to provide information to regional manners, sub-catchments were established according to the order in which they require treatment

using conservation technologies based on the amount of soil loss [61–64]. The highest priority for soil conservation treatments is given to upland catchments that have the highest soil loss (Figure 4).

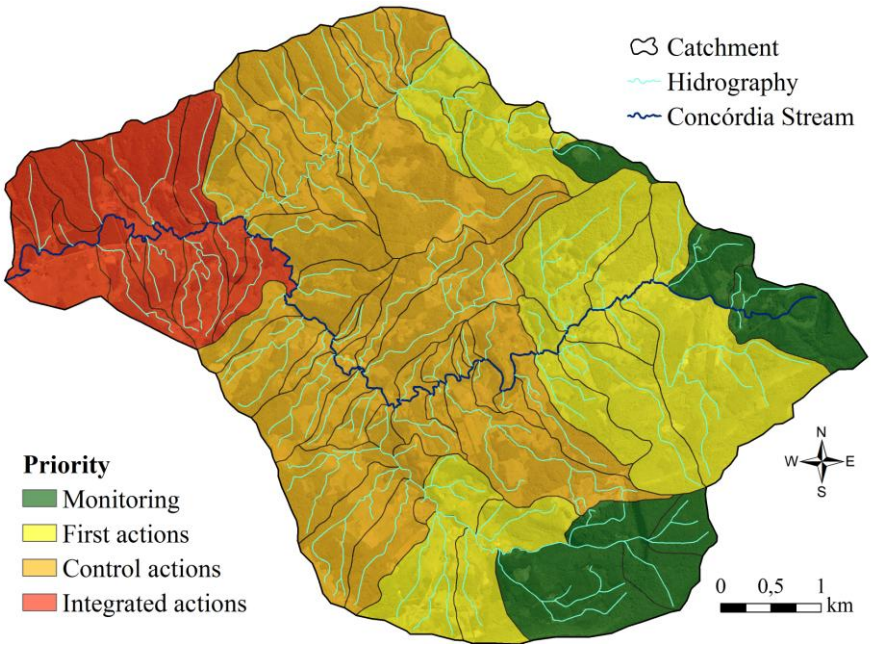

Figure 4. Priority map of Concordia River catchment, Lontras, Santa Catarina, Brazil.

For the upland areas of the catchment, we suggest only water monitoring in order to identify natural processes. The next priority is to instruct family farmers to apply simple techniques to reduce erosion processes on small properties. The next task is a complex action because this area comprises the agricultural part of the catchment. Control actions should be applied in this region to reduce erosion processes and consequently the sediment load in the river. The outflow area requires integrated actions that encompass the entire catchment. If previous actions had been applied adequately, this section would not be a problem, as the sediments resulting from agricultural practices area mostly controlled.

4. Conclusions

GIS can be easily used to treat digital georeferenced data that can be used to assess areas vulnerable to erosion, even in fragmented agricultural catchments. The studied catchment is representative of the situation in the state of Santa Catarina, particularly the eastern part that consists of a large number of small agricultural catchments where family farming using conventional systems predominates. USLE and field measurements have the potential to be applied in various state cases. We support the use of this methodology in small municipalities for which digital data is easily accessible at http://sigsc.sds.sc.gov.br/, where 70,000 colored and infrared images and digital models

are available at high spatial resolution. GIS becomes important when there is a lack of information or when the area is difficult to access. Using GIS, vulnerability maps can be drawn to facilitate initial decision making. However, we emphasize the use of field sampling. Otherwise, it is recommended that the sampling points have adequate spatial spread in the catchment area. The results of this study encourage the use of this tool to assist local and state decision makers to easily assess the areas vulnerable to erosion and to promote action to help reduce the impact of agricultural activities.

Another point to be highlighted is related to the importance of monitoring flow, suspended solids, and drag. This data could be used to make inferences about erosion. As stated in the literature, only 25% of the available sediment reaches the main river and the outflow of the catchment. The season with the highest vulnerability of soil loss is summer, followed by fall and spring. Conventional tillage used for summer crops has led to increased vulnerability, thus increasing turbidity levels in the river. Of the soil types, Gleysol Haplic Ta aluminic and Cambisol humic aluminic are particularly vulnerable, especially in summer.

Acknowledgements

Authors acknowledge CNPq and CAPES for the research grant.

Conflict of Interest

All authors declare no conflicts of interest in this paper.

References

1. Silva AM, Silva MLN, Curi N, et al. (2005) Perdas de solo, água, nutrientes e carbono orgânico em Cambissolo e Latossolo sob chuva natural. *Pesq Agrop Bra* 40: 1223-1230.
2. Karydas C, Sekuloska T, Silleos G (2009) Quantification and site-specification of the support practice factor when mapping soil erosion risk associated with olive plantations in the Mediterranean island of Crete. *Environ Monit Assess* 149: 19-28.
3. Ganasri BP, Ramesh H (2015) Assessment of soil erosion by RUSLE model using remote sensing and GIS—A case study of Nethravathi Basin. *Geosc Front*: 1-9.
4. Lin BS, Thomas K, Chen CK, et al. (2016) Evaluation of soil erosion risk for watershed management in Shenmu watershed, central Taiwan using USLE model parameters. *Paddy Water Environ* 14: 19-43.
5. Markose VJ, Jayappa KS (2016) Soil loss estimation and prioritization of sub-watersheds of Kali River basin, Karnataka, India, using RUSLE and GIS. *Environ Monit Assess*: 188-225.

6. Rahman MR, Shi ZH, Chong C (2009) Soil erosion hazard evaluation: an integrated use of remote sensing, GIS and statistical approaches with biophysical parameters towards management strategies. *Ecol Modell* 220: 1724-1734.
7. Peter HBC, Chandler JH, Armstrong A (2010) Applying close range digital photogrammetry in soil erosion studies. *Photogramm Rec* 25: 240-265.
8. Wischmeier WH, Smith DD (1965) Predicting Rainfall-Erosion Losses from Gopland East of the Rocky Mountains. *Agri Hand* 282: 47.
9. Strand RI, Pemberton EL (1982) *Reservoir sedimentation: Technical guidelines for Bureau of Reclamation*. U.S. Bureau of Reclamation, Denver.
10. Ananda J, Herath G (2003) Soil erosion in developing countries: a socio-economic appraisal. *J Environ Manag* 68: 343-353.
11. Humberto BC, Rattan L (2008) Water erosion. In: *Principles of soil conservation and management*. Springer, New York, 21-53.
12. Jinren RN, Yingkui KL (2003) Approach to soil erosion assessment in terms of land-use structure changes. *J Soil Water Conserv* 58: 158-169.
13. Prasannakumar V, Shiny R, Geetha N, et al. (2011) Spatial prediction of soil erosion risk by remote sensing, GIS and RUSLE approach: A case study of Siruvani River watershed in Attapady valley, Kerala, India. *Envir Ear Sc* 64: 965-972.
14. Chen T, Niu R, Ni P, et al. (2011) Regional soil erosion risk mapping using RUSLE, GIS, and remote sensing: A case study in Miyun Watershed, North China. *Envir Ear Sc* 63: 533-541.
15. Beskow S, Mello CR, Norton LD, et al. (2009) Soil erosion prediction in the Grande River Basin. Brazil using distributed modeling. *Catena* 79: 49-59.
16. Cohen MJ, Shepherd KD, Walsh MG (2005) Empirical reformulation of the universal soil loss equation for erosion risk assessment in a tropical watershed. *Geoderma* 124: 235-252.
17. Werneck Lima JEF, Lopes WTA, Aquino FG, et al. (2014) Assessing the use of erosion modeling to support payment for environmental services programs. *J of Soils and Sed* 14: 1258-1265.
18. Mellerowicz KT, Rees HW, Chow TL, et al. (1994) Soil conservation planning at the watershed level using the Universal Soil Loss Equation with GIS and microcomputer technologies: a case study. *J Soil Water Conser* 49: 194-200.
19. Ha NM (2011) Application of USLE and GIS tool to predict soil erosion potential and proposal land cover solutions to reduce soil loss in Tay Nguyen. *FIG Conference—Bridging the Gap Between Cultures*—Marrakech, Morocco.
20. Karydas CG, Sekuloska T, Sarakiotis I (2005) Fine scale mapping of agricultural landscape features to be used in environmental risk assessment in an olive cultivation area. *IASME Trans* 2: 582-589.
21. Mati BM, Veihe A (2001) Application of the USLE in a savannah environment: comparative experiences from East and West Africa. *Singap J Trop Geogr* 22: 138-155.

22. Angima SD, Stott DE, O'Neill MK, et al. (2003) Soil erosion prediction using RUSLE for central Kenyan highland conditions. *Agric Ecosyst Environ* 97: 295-308.
23. Kothyari UC, Tewari AK, Singh R (1994) Prediction of sediment yield. *J of Irrig and Drain Eng ASCE* 120: 1122-1131.
24. Pandolfo C, Braga HJ, Silva Junior VP, et al. (2002) *Atlas climático digital do Estado de Santa Catarina.* Florianópolis: Epagri. CD-Rom.
25. Pinheiro A, Kaufmann V, Perazzoli M, et al. (2010) Avaliação dos escoamentos em diferentes escalas espaciais na bacia do ribeirão Concórdia [Evaluation of flows in diferentes patialscales in the Concórdia creek basin]. In *X Symposium of Water Resources of Nordeste*, Fortaleza 1: 1-11. Porto Alegre Brazil: ABRH.
26. Klein RM, Rodriguez HB (1978) Mapa Fitogeográfico do Estado de Santa Catarina [Phytogeographic map of the state of Santa Catarina]. In *Mapa Fitogeográfico do Estado de Santa Catarina*. Imprensa Oficial do Estado de Santa Catarina. IOESC. Florianópolis, SC, Brazil.
27. Wischmeier WH, Smith DD (1978) Predicting rainfall erosion losses: a guide to conservation planning. *Agric Handb* 537, Washington-D.C: USDA. 57 p.
28. Renard KG, Freimund JR (1994) Using monthly precipitation data to estimate the R-factor in the reviser USLE. *J of Hydr* 157: 287-306.
29. Kim JB, Saunders P, Finn JT (2005) Rapid Assessment of soil erosion in the rio Lempa Basin, Central America, Using the Universal Soil Loss equation and Geographic Information Systems. *Envir Manag* 36: 872-885.
30. Bertoni J, Lombardi Neto F (1998) *Conservação do solo.* 4. ed. São Paulo: Ícone Ed., 392 p.
31. Denardin JE (1990) *Erodibilidade de solo estimada por meio de parâmetros físicos e químicos*. 81p. Thesis (Doctored em Agronomy—Soil and Nutrition of Plants)—Escola Superior de Agricultura Luiz de Queiroz, Univ. de São Paulo, Piracicaba.
32. Caputo HP (1988) *Mecânica dos Solos e suas aplicações*. Fundamentos. 6º edição, Rio de Janeiro: Livros Técnicos e Científicos Editora.
33. Galindo ICL, Margolis E (1989) Tolerância de perdas por erosão para solos do Estado de Pernambuco. *Rev Bra de Ciê do Solo* 13: 95-100.
34. Alexakis DD, Hadjimitsis DG, Agapiou A (2013) Integrated use of remote sensing, GIS and precipitation data for the assessment of soil erosion rate in the catchment area of "Yialias" in Cyprus. *Atm Resea* 131: 108-124.
35. Ranzi R, Hung Le T, Rulli MC (2012) A RUSLE approach to model suspended sediment load in the Lo River (Vietnam): effects of reservoirs and land use changes. *J of Hydrol*: 422-423.
36. Paiva EMC, Paiva JBD (2001) *Hidrologia aplicada à gestão de pequenas bacias hidrográficas*. Porto Alegre: ABRH, 367 p.
37. Williams JR, Berndt HD (1977) Determining the universal soil equation`s length-slop factor for watershed. In: *Soil Erosion: prediction and control*. Ankeny: Soil Conservation Society of America: 217-255.

38. Bertol I, Shick J, Batistela O (2002) Razão de perdas de solo e Fator C para milho e aveia em rotação com outras culturas em três tipos de preparo de solo. *Rev Bra de Ciê de Solo* 26: 545-552.
39. Martins SG, Silva MLN, Avanzi JC, et al. (2010) Fator cobertura e manejo do solo e perdas de solo e água em cultivo de eucalipto e em Mata Atlântica nos Tabuleiros Costeiros do Estado do Espírito Santo. *Scien. Forest* 38: 517-526.
40. Stein DP, Donzelli PL, Gimenez AF, et al. (1987) Potencial de erosão laminar, natural e antrópico, na Bacia do Peixe-Paranapanema. *Anais 4 ºSimpósio Nacional de Controle de Erosão*. Marília-SP: ABGE/DAEE: 105-135.
41. Tomzani JC, Mantovani LE, Bittencourt AVL, et al. (2005) Sistematização dos fatores da Eups em SIG para quantificação da erosão laminar na bacia do rio Anta Gorda (PR). *Est Geog* 3: 1-21.
42. Morgan RPC (1995) *Soil erosion and Conservation*. Longman Group Limited, 2 ed.
43. Silva AM, Schulz HE, Camargo PB (2007) *Erosão e hidrossedimentologia em bacias hidrográficas*. 2. Ed. São Carlos-SP: RiMa, 158 p.
44. Strand GH, Dramstad W, Engan G (2002) The effect of field experience on the accuracy of identifying land cover types in aerial photographs. *Int J Appl Earth Obs Geoinf* 4: 137-146.
45. Wanielista MP (1978) *Storm water management: quality and quantity*, Ann Arbor Science, 383 p.
46. Ali SA, Hagos H (2016) Estimation of soil erosion using USLE and GIS in Awassa catchment, Rift valley, Central Ethiopia. *Geod Reg* 7: 159-166.
47. Berberoglu S (2003) Sustainable management for the Eastern Mediterranean coast of Turkey. *Env Manag* 31: 442-451.
48. Ali SA, Tesgaya D (2010) Landuse and landcover change detection between 1985–2005 in parts of Highland of Eastern Ethiopia using remote sensing and GIS techniques. *Int J Geoinf* 6: 35-40.
49. Meshesha DT, Tsunekawa A, Tsubo M, et al. (2014) Land use change and its socio-environmental impact in Eastern Ethiopia's Highland. *Reg Environ Chang* 14: 757-768.
50. Evrendilek F, Doygun H (2000) Assessing major ecosystem types and the challenge of sustainability in Turkey. *Env Manag* 26: 479-489.
51. Wali MK, Safaya NM, Evrendilek F (2002) Ecological rehabilitation and restoration in the Americas with special reference to the United States of America. In: Perrow MR, Davy AJ (Eds.) *Handbook of Rest Ec* 2. Cambridge University Press, Cambridge, 3-31.
52. Yang CT (1996) *Sediment Transport: Theory and Practice.* McGraw-Hill Book Company, Inc, New York.
53. EMBRAPA (1997) *Manual de métodos de análise de solo*. Rio de Janeiro. 2. ed. rev. EMBRAPA: 212 p.
54. Yang CT (1973) Incipient motion and sediment transport. *J of the Hyd Div* 99: 1679-1701.
55. Silva CR, Bressiani DA, Bettiol GM S, et al. (2014) Aplicação do Modelo SWAT (Soil and Water Assessment Tool) para estimar produção de sedimento e nutrientes na Microbacia Experimental da EMBRAPA Pecuária Sudeste. *Simpósio Nacional de Instrumentação Agropecuária*. São Carlos: 609-612.

56. Silva CR (2010) *Aplicação do Modelo SWAT para estimar produção de sedimentos e transporte de fósforo e nitrogênio na microbacia do Ribeirão Canchim—EMBRAPA Pecuária Sudeste.* Dissertação (Mestrado)—Escola de Engenharia de São Carlos, Universidade de São Paulo, São Carlos.
57. Vieira VF (2008) Estimativa de perdas de solo por erosão hídrica em uma sub-bacia hidrográfica. *Geografia* 17: 73-81.
58. Oliveira VA, Mello CR, Durães MF, et al. (2014) Vulnerabilidade a erosão do solo na bacia do rio Verde, Minas Gerais do Sul. *Ciê Agrotec* 38.
59. Pradeep GS, Ninu Krishnan MV, Vijith H (2014) Identification of critical soil erosion prone areas and annual average soil loss in an upland agricultural watershed of Western Ghats, using analytical hierarchy process (AHP) and RUSLE techniques. *Arab J of Geosc* 8: 3697-3711.
60. Gilles L, Cogo NP, Bissani CA, et al. (2009) Perdas de água, solo, matéria orgânica e nutriente por erosão hídrica na cultura do milho implantada em área de campo nativo, influenciadas por métodos de preparo do solo e tipos de adubação. *Rev Bra de Ciê do Solo* 33, p. 1427-1440.
61. Adinarayana J (2003) Spatial decision support system for identifying priority sites for watershed management schemes. In *First interagency conference on research in the watersheds* (ICRW) Arizona: Benson: 405-408.
62. Silva RM, Santos CAG, Montenegro SMGL (2012). Integration of GIS and remote sensing for estimation of soil loss and prioritization of critical sub-catchments: a case study of Tapacura catchment. *Nat Haz* 62: 953-970.
63. Patel DP, Gajjar CA, Srivastava PK (2013) Prioritization of Malesari mini-watersheds through morphometric analysis: a remote sensing and GIS perspective. *Env Ear Sc* 69: 2643-2656.
64. Khadse GK, Vijay R, Labhasetwar PK (2015) Prioritization of catchments based on soil erosion using remote sensing and GIS. *Env Monit and Assess* 187: 333.

AIMS Press